Exploiting evanescent-wave amplification for subwavelength low-contrast particle detection

Roy, S.; Pereira, S. F.; Urbach, H. P.; Wei, Xukang; El Gawhary, O.

DOI
10.1103/PhysRevA.96.013814

Publication date
2017

Document Version
Final published version

Published in
Physical Review A (Atomic, Molecular and Optical Physics)

Exploiting evanescent-wave amplification for subwavelength low-contrast particle detection

S. Roy,[1] S. F. Pereira,[1,*] H. P. Urbach,[1] Xukang Wei,[1,†] and O. El Gawhary[1,2]
[1]*Department of Imaging Physics, Delft University of Technology, Lorentzweg 1, 2628 CJ Delft, Netherlands*
[2]*VSL Dutch Metrology Institute, Thijsseweg 11, 2629 JA Delft, Netherlands*
(Received 29 November 2016; published 10 July 2017)

The classical problem of subwavelength particle detection on a flat surface is especially challenging when the refractive index of the particle is close to that of the substrate. We demonstrate a method to improve the detection ability several times for such a situation, by enhancing the "forbidden" evanescent waves in the substrate using the principle of super-resolution with evanescent waves amplification. The working mechanism of the system and experimental validation from a design with a thin single dielectric layer is presented. The resulting system is a simple but complete example of evanescent-wave generation, amplification, and the consequent modulation of the far field. This principle can have far reaching impact in the field of particle detection in several applications ranging from contamination control to interferometric scattering microscopy for biological samples.

DOI: 10.1103/PhysRevA.96.013814

The study of negative refractive index materials was initiated by Veselago [1] to understand whether such materials would, from a purely theoretical point of view, violate the founding laws of physics. A significant increase in interest among the research community in this subject occurred when Pendry [2] suggested that those materials would be capable of amplifying evanescent waves and eventually lead to unlimited spatial resolution. The crux of Pendry's method was the use of a layer of negative-index media for restoration of otherwise damped evanescent waves. However, it has been shown from a theoretical viewpoint [3] that a slab of such a material works only if object and detector are both in the near field [4–6]. Far-field imaging with the evanescent-wave amplification has also been shown [7–11], for example, utilizing far-field superlenses and anisotropic metamaterials, although neither of these techniques had a simple construction like a thin slab. Alternatively, some authors [12,13] have doubted the mechanism of evanescent-wave amplification as detailed in Ref. [2]. It was, in fact, later shown that a dielectric layer is capable of doing similar amplification [14–16] for both parallel (p) and perpendicular (s) polarization, essentially triggering Fabry–Perot-like resonances. The existence of evanescent-wave amplification also for s-polarized light rules out the interpretation of the super-resolution effects through mimicking negative refraction in metals, as suggested in Ref. [2], because that case simply falls outside the theoretical framework of the negative-index-materials theory. Moving to dielectrics layers offers some simplicity from a fabrication point of view, especially on a large scale. However, these dielectric layers are also only effective in the near field on their own.

There has been little attention on using this principle for a problem which can significantly benefit from this concept: particle detection on a flat substrate. This problem is critical for substrate quality inspection in many important fields, such as semiconductors, organic polymers, optical-component manufacturing, the nanofabrication industry [17,18], and biological microscopy with nanoparticle markers, such as interferometric scattering microscopy [19]. Novotny showed that the "forbidden light" [20,21], i.e., light emitted by a dipole scatterer into supercritical angles inside the planar substrate under it [22], contains a significant amount of information about the scatterer. Although particle detection by evanescent waves is well known [23–25], the effect of using amplified evanescent waves for particle detection on a planar substrate is not well researched. A possible reason is the necessity of bringing the device converting the amplified evanescent waves into detectable far-field modulations very close to the sample. This is inconvenient for practical use and also is a source of further contamination. Thus, it is desired to have the evanescent modes originating from the particle to get amplified and detected in the far field without the presence of anything other than the amplifying media in the near field, combining both the ideas into "amplified forbidden light" with a practical and useful design.

We investigate here the effects of evanescent-wave amplification for detection of particles on a flat substrate coated with a very thin ($\approx\lambda/30$) evanescent-wave amplifying layer. We consider subwavelength particles which are almost perfectly index matched to the substrate, which is a challenging situation for particle detection [26,27], and show that the detection sensitivity is significantly improved (almost 500% signal-to-noise improvement). This implies that, by this technique, compared with the not-enhanced case, particles that are nearly undetectable can be clearly detected. We present the working mechanism and numerical analysis of the principle, followed by experimental validation.

The evanescent waves, which are produced by a probe interacting with a target, are usually not available in a technique when the detector is located in the far field. In our case the optical probe consists of a field focused by a microscope objective and contains no evanescent waves. The way we circumvent this limitation and still exploit the advantages of near-field optics, is by using the evanescent part of the field scattered by the target itself, when illuminated by the incident optical field, as a new secondary optical probe. To realize this all one needs to do is to modify the properties of the physical support where the target is placed in a way that a large part of the evanescent waves generated

*s.f.pereira@tudelft.nl
†On leave from the School of Physics, Nankai University, Tianjin 300071, China.

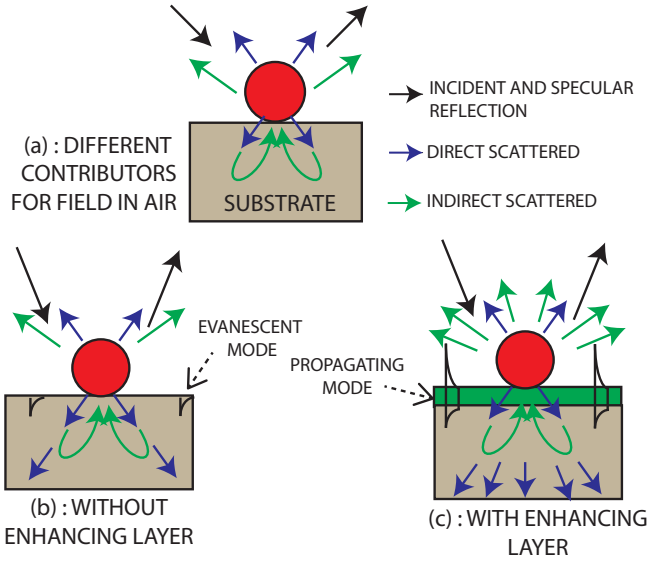

FIG. 1. The mechanism of enhancement of evanescent waves and particle detection. (a) The main constituents of the outgoing field in air for a particle on a substrate in air. In the normal case (b), the incident field is scattered by the particle, but the evanescent modes decay quickly in the substrate and in air. It does not contribute significantly when they are rescattered to propagating modes in air. The situation changes when the evanescent modes are amplified (c) by a thin enhancing layer and the scattered field is boosted by a large contribution from rescattered evanescent waves. As indicated in panel (c), the enhancement results in increase in field at the substrate side as well. The z axis coincides with the optical axis of scanning system, with $z > 0$ in air, and $z = 0$ at air interface.

by the scattering process between target and incident field is reflected back by the support and redirected towards the scatterer. Depending on the support, this secondary probe, containing evanescent waves this time, interacts again with the target and the new scattered field can be recorded in the far field. More importantly, the support can be realized in such a way that the amplitude of the evanescent waves, produced by the first interaction between target and incident field, is actually increased, resulting in an improved signal-to-noise ratio (SNR) of the recorded signal. In our work, the target is represented by small dielectric particle on a flat substrate which is illuminated by a focused optical field. The resulting scattered field is recorded by a detector placed in the far field. Generally speaking, once illuminated by a focused field, the scattered field in a specific direction consists of mainly three components [28], as shown in Fig. 1(a). These are (1) the specular reflection, mostly due to the interaction of the incident field with the bare substrate only, (2) the direct scattered field, produced by the scattering between particle and incident field, and (3) a indirect scattered field, produced by the interaction of the direct scattered field with the substrate and rescattered by the particle. This reflected scattered field, being the secondary probe, is essentially reflected back and can be eventually amplified by the substrate. For an isolated small particle, a large amount of the scattered waves are evanescent, and so they do not directly reach the detector. It is possible to recover some of those waves by amplifying them and then letting the particle rescatter them into propagating modes. The steps of the working mechanism in short are as follows:

(i) The illuminating field is first scattered by the nanoparticle which generates the evanescent field. Some of the scattered field propagates from the particle towards the substrate.

(ii) Propagating and evanescent waves, directed towards the substrate, hit the substrate. This interaction gives rise to a reflected field, which still contains propagating and evanescent waves. The substrate can eventually modify the amplitude of the waves and enhance the amplitude of evanescent waves. With proper design, the enhancing layer can be made to have a good Q factor with large full width at half maximum (FWHM), so that a broad band of spatial frequencies can be amplified.

(iii) Such a back-reflected field interacts again with the particle and gives rise to a new scattering process.

(iv) The scattered field is collected by the detector.

In this construction, the particle not only represents the target but also plays the role of the seed for evanescent-wave generation, and the waves are further enhanced by the engineered substrate.

To verify the feasibility of such approach, two samples were prepared. On the first sample, polystyrene latex (PSL), particles 200 nm diameter were deposited on a flat glass plate (UV grade fused silica, flatness less than 20 nm, 5 mm thick). The second one was a 600 μm glass plate of the same material with a layer of 20 nm InSb on top, which functions as an evanescent-wave enhancing layer. The thickness of the evanescent-wave enhancing layer is less critical for us than situations where spatially narrow-band evanescent waves are generated by the object which needs to be amplified, such as in the case of the grating studied in Ref. [5]. To show that this specific layer can function as an enhancement layer for evanescent waves, simulations were performed. The simulations were done in two steps. At first, an analytic but rigorous model [29] was used to verify the response of thin film stack only, without any scatterer. In Figs. 2(a)–2(d), the modulus of the complex reflectance as a function of normalized wave vector (k_x/k_{air}) and distance z from the air-substrate interface is shown. The enhancement of evanescent modes can be seen if Figs 2(a) and 2(b) are compared with Figs. 2(c) and 2(d). The enhancement is larger for an s-polarized field, which is more clearly seen from Fig. 2(g), where the difference between the amplitudes of the complex reflection coefficients of enhanced and not-enhanced samples are plotted for a specific distance from the air interface ($z = 10$ nm). This metric shows the comparison of amplification of two amplifiers, without and with enhancing layer, for each polarization as a function of spatial frequency. A positive value of this difference for approximately $1.4 \leqslant k_x/k_{\text{air}} \leqslant 5$ indicates that the amplification of the enhanced sample is better. The peak amplification is around $k_x/k_{\text{air}} = 1.8$, for s-polarized light, with about 60% enhancement. This indicates that the design is capable of amplifying evanescent waves in the near field and as a result can produce a higher SNR compared with the standard sample without enhancing layer. To verify the assumptions yet more rigorously, a model of the actual experimental arrangement was created by using the finite element method (FEM) [30], and the x-polarized electric-field distribution in the x-z plane is shown for a not-enhanced [Fig. 2(h)] and enhanced [Fig. 2(i)] sample. Simulations are

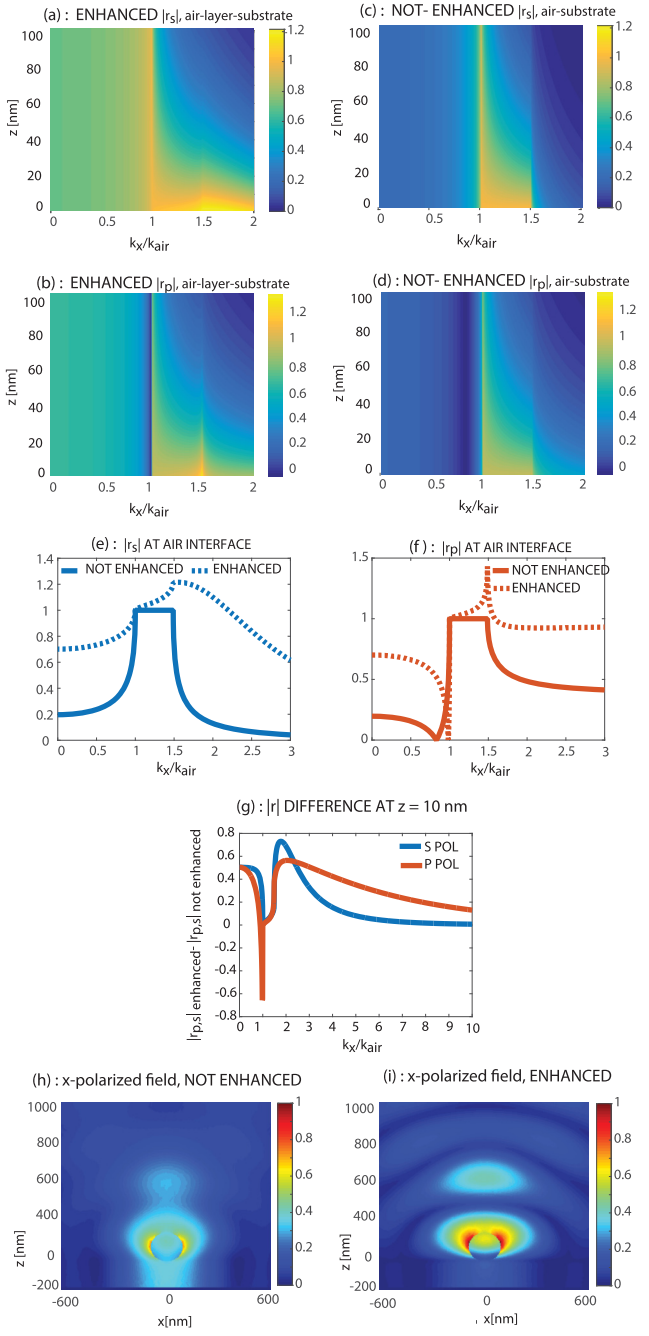

FIG. 2. The modulus of reflectance ($|r|$) for parallel (p) and perpendicular (s) polarized waves are simulated respectively for a substrate (a), (b) with and (c), (d) without enhancement layer of InSb. In each case the reflectance is shown against the normalized x component of the wave vector (k_x/k_{air}) and the distance z from the air interface. In panels (e) and (f), the variation of $|r|$ with wave vector at the air-interface ($z = 0$) is shown. The Brewster's angle for air-glass interface is seen at z at $k_x/k_{\text{air}} \approx 0.82$ in panel (f). The effect of evanescent-wave amplification by the InSb layer is clearly seen from panels (e) and (f). In panel (g), the differences between the $|r|$ for enhanced and not-enhanced samples are plotted for each polarization with k_x/k_{air} for $z = 10$ nm. This value of z was chosen arbitrarily, since the particle will scatter light over a large range of z ($0 \leqslant z \leqslant 200$ nm). In panels (h) and (i) the x-polarized electric field, in the x-z plane, is shown when a focused x-polarized beam is incident on the sample-air interface.

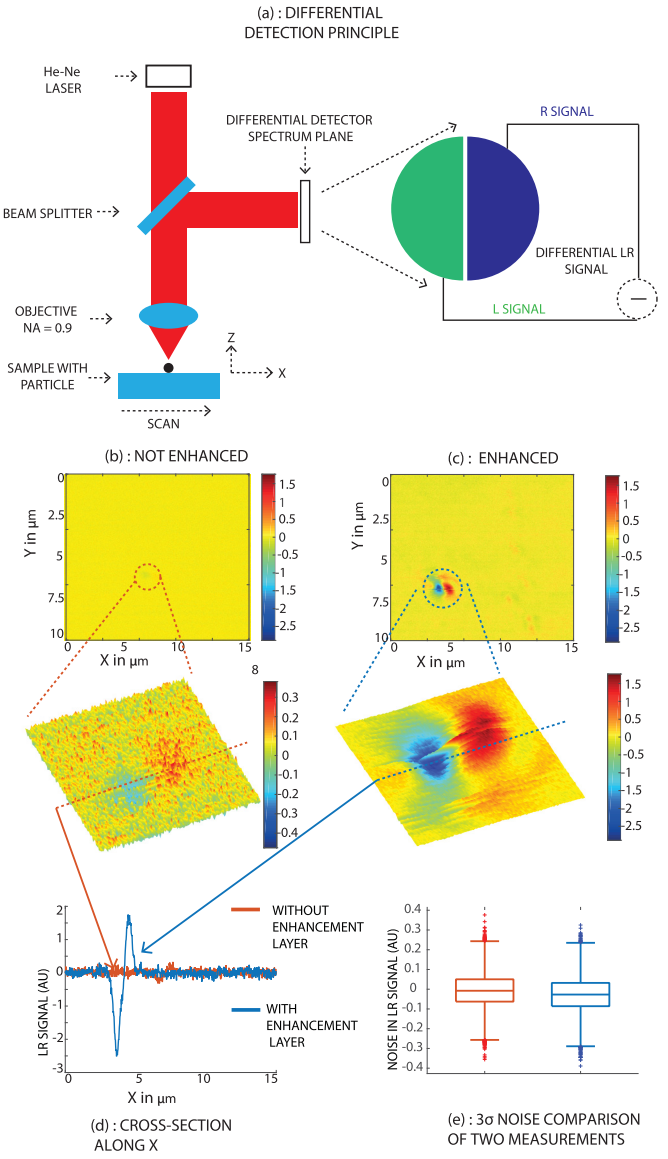

FIG. 3. The differential detection principle is shown in panel (a). In panels (b) and (c) the far-field maps of the sample without and with the enhancement layer are shown. The figures under panels (b) and (c) show the three-dimensional view of the signal maps near the particle. Please note the change in scale for the not-enhanced case, which is necessary to show the signal from the particle. (d) Signals can be quantitatively compared by plotting the cross sections. The noise of the two measurements are compared in panel (e), which have mean $+3\sigma \approx -0.09 + 0.42$ (without enhancement layer) and $-0.2 + 0.42$ (with enhancement layer). Particle localization is not possible without the enhancement layer.

shown for each substrate (enhanced and not-enhanced), in accordance with the coordinate system described in Fig. 1, using a simulation volume of 1.3 μm^3. We used an InSb layer and substrate refractive index $4.28 + 1.81i$ and 1.48. Particle material refractive index was 1.58. While both the plots use the same scale, a visual inspection clearly shows the effect of the enhancing layer. The choice of x-z plane is only for representation; the final effect, when all the other planes are considered, will be much larger.

To make a fair comparison between the two samples it is necessary to eliminate the effect of the increased background reflection level resulting from the increase in reflectance for the propagating modes ($k_x < k_{\text{air}}$) when the layer is present. For this, differential detection is performed by subtraction of the detected intensities in the two halves of the detector [Fig. 3(a)]. To do this, linearly polarized He-Ne laser light ($\lambda = 632$ nm) is incident onto an objective with numerical aperture (NA) of 0.9 was used to focus the light on the air-substrate interface. The substrate is scanned in the lateral (x-y) direction and the reflected light is captured by the same objective. A beam splitter was used to divert the outgoing field such that the back focal plane (spectrum plane) is captured by a differential silicon detector [Fig. 3(a)]. The sample was placed on a Physik Instrumente piezo-electric actuator operating within its linear range. The actuator can move the sample in the x-y plane [31,32].

With this differential detection principle the source power variation is no longer a problem, also, the localization accuracy and SNR with differential detection is significantly higher even with a low incident power and relatively fast signal acquisition. Most importantly, this differential signal (LR signal) is independent of substrate reflectance, as can be seen from of Figs. 3(b) and 3(c). Scanning was repeated for both the samples with identical power level, temperature, and other experimental conditions.

The LR signal maps in Figs 3(b) and 3(c) show the corresponding variations of the signal as the sample is scanned without and with the enhancement layer, respectively (on the same scale). In both cases, the data with the maximum SNR, obtained after measurements with several randomly chosen particles, are compared. From the results, it is seen that the particle is hardly detected in Fig. 3(b), whereas it is clearly detected in Fig 3(c). The surface plots below the respective figures shows the vicinity of the particle. Please note the magnified scale used to show clearly the particle when the enhancing layer is absent. The increase in SNR can be seen more clearly if a cross section is taken, which is shown in Fig. 3(d). The modulation (max-min) increases by a factor of 5.47 with the application of the layer. The difference in modulation is seen in the surface plots mentioned before. To be noted, because of the differential detection, the signal amplitude does not change between the two samples unless the particle is in the vicinity. That is why away from the particle the signal is close to zero for both cases. This is shown more clearly in Fig. 3(e), where comparison of noise between two measurements are shown. The mean noise values for two cases are -0.09 (without enhancement layer) and -0.2 (with enhancement layer). The noise standard deviation is 0.16 for both cases. When needed, this standard deviation also determines the uncertainty in localization of the center of the particle which can be determined when the signal between the positive and negative peaks [Fig. 3(d)] is equal to the noise. With the enhancement layer, the uncertainty of localization is 30 nm, while without the enhancement layer, localization is not possible (3σ noise $>$ signal).

In this article, we demonstrate how the detection sensitivity of particles on a substrate is highly enhanced by using the principle of evanescent-wave amplification. We develop it by merging the benefits of two well-known principles: evanescent-wave amplification by dielectric slabs and detection of scatterers using forbidden evanescent modes. This technique can be especially useful to detect index-matched subwavelength particles, which is always an issue in many technologies that require nanoparticle detection. A successful demonstration of the technique is presented. The basic principles explained here can be extended in several ways. Depending on the application, one can fabricate suitable enhancing layers which are more optimized for the situation. For example, a properly chosen material for the barrier or protective layer for organic polymers [33], applied to prevent substrate degradation, can doubly function as an enhancing layer. Alternatively, for particle detection on substrates such as particle tracking, a multilayered stack can achieve broadband evanescent-wave amplification, yielding an enhancement of detection sensitivity for several wavelengths. The amplification due to the guided mode is polarization dependent, so a suitable polarization scheme, such as radially polarized illumination [34], can be used for an enhancing layer designed to amplify p-polarized light, giving a better SNR due to elimination of the polarization component which is not amplified.

The authors acknowledge Roland Horsten and Thim Zuidwijk of the Delft University of Technology for the electronics and mechanical design of the experimental system. Christiaan Hollemans of TNO, Delft is acknowledged for his contribution in preparing the samples. S. Roy acknowledges the Seventh Framework Program (No. FP7/2007-2013 of the European Union) under Grant Agreement No. 281027 for funding. Xukang Wei acknowledges the School of Physics, Nankai University for financing his stay in the Netherlands.

[1] V. G. Veselago, Sov. Phys. Usp. **10**, 509 (1968).
[2] J. B. Pendry, Phys. Rev. Lett. **85**, 3966 (2000).
[3] V. A. Podolskiy and E. E. Narimanov, Opt. Lett. **30**, 75 (2005).
[4] P. V. Parimi, W. T. Lu, P. Vodo, and S. Sridhar, Nature (London) **426**, 404 (2003).
[5] N. Fang, H. Lee, C. Sun, and X. Zhang, Science **308**, 534 (2005).
[6] Strictly speaking, we should say when the distance between object and image plane is twice the distance of the thickness of the amplifying slab.
[7] S. Durant, Z. Liu, J. M. Steele, and X. Zhang, J. Opt. Soc. Am. B **23**, 2383 (2006).
[8] Z. Liu, S. Durant, H. Lee, Y. Pikus, N. Fang, Y. Xiong, C. Sun, and X. Zhang, Nano Lett. **7**, 403 (2007).
[9] A. Salandrino and N. Engheta, Phys. Rev. B **74**, 075103 (2006).
[10] I. I. Smolyaninov, Y.-J. Hung, and C. C. Davis, Science **315**, 1699 (2007).
[11] Z. Liu, H. Lee, Y. Xiong, C. Sun, and X. Zhang, Science **315**, 1686 (2007).

[12] R. W. Ziolkowski and E. Heyman, Phys. Rev. E **64**, 056625 (2001).
[13] G. Christou and C. Mias, Plasmonics **6**, 307 (2011).
[14] O. E. Gawhary, N. J. Schilder, A. da Costa Assafrao, S. F. Pereira, and H. P. Urbach, New J. Phys. **14**, 053025 (2012).
[15] C. J. Regan, D. Dominguez, L. G. de Peralta, and A. A. Bernussi, J. Appl. Phys. **113**, 183105 (2013).
[16] R. Lopez-Boada, C. J. Regan, D. Dominguez, A. A. Bernussi, and L. G. de Peralta, Opt. Express **21**, 11928 (2013).
[17] A. Okamoto, H. Kuniyasu, and T. Hattori, IEEE Trans. Semicond. Manuf. **19**, 372 (2006).
[18] A. Chen, V. Huang, S. Chen, C. J. Tsai, K. Wu, H. Zhang, K. Sun, J. Saito, H. Chen, D. Hu, M. Li, W. Shen, and U. Mahajan, Proc. SPIE **7140**, 71400W (2008).
[19] J. Ortega-Arroyo and P. Kukura, Phys. Chem. Chem. Phys. **14**, 15625 (2012).
[20] L. Novotny, J. Opt. Soc. Am. A **14**, 105 (1997).
[21] L. Novotny and B. Hecht, in *Principles of Nano-Optics*, 1st ed. (Cambridge University Press, Cambridge, 2006), pp. 336–338.
[22] N. Dahan and J.-J. Greffet, Opt. Express **20**, A530 (2012).
[23] E.-H. Lee, R. E. Benner, J. B. Fenn, and R. K. Chang, Appl. Opt. **18**, 862 (1979).
[24] C. Zettner and M. Yoda, Exp. Fluids **34**, 115 (2003).
[25] J. S. Guasto and K. S. Breuer, Exp. Fluids **47**, 1059 (2009).
[26] G. G. Daaboul, C. A. Lopez, J. Chinnala, B. B. Goldberg, J. H. Connor, and M. S. Ünlü, ACS Nano **8**, 6047 (2014).
[27] O. Avci, M. I. Campana, C. Yurdakul, and M. S. Ünlü, Optica **4**, 247 (2017).
[28] S. Roy, K. Ushakova, Q. van den Berg, S. F. Pereira, and H. P. Urbach, Phys. Rev. Lett. **114**, 103903 (2015).
[29] O. E. Gawhary, M. C. Dheur, S. F. Pereira, and J. J. M. Braat, Appl. Phys. B: Lasers Opt. **111**, 637 (2013).
[30] X. Wei, A. J. Wachters, and H. P. Urbach, J. Opt. Soc. Am. A **24**, 866 (2007).
[31] S. Roy, A. C. Assafrao, S. F. Pereira, and H. P. Urbach, Opt. Express **22**, 13250 (2014).
[32] S. Roy, M. Bouwens, L. Wei, S. F. Pereira, H. P. Urbach, and P. van der Walle, Rev. Sci. Instrum. **86**, 123111 (2015).
[33] J. Pospíšil and S. Nešpurek, Prog. Polym. Sci. **25**, 1261 (2000).
[34] R. Dorn, S. Quabis, and G. Leuchs, Phys. Rev. Lett. **91**, 233901 (2003).